Assessment of a grain oriented wound core transformer for solid state converter

Houssam Ichou, Daniel Roger, Mathieu Rossi, Thierry Belgrand, Regis Lemaitre

Version of Record: https://www.sciencedirect.com/science/article/pii/S0304885319328215
Manuscript_8e70a8a67af8c1610361afdd63f21985

Assessment of a grain oriented wound core transformer for solid state converter

Houssam Ichou[a,*], Daniel Roger[a], Mathieu Rossi[a], Thierry Belgrand[b] and Regis Lemaitre[b]

[a] Univ. Artois, EA4025, LSEE, 62400 Béthune, France
[b] thyssenkrupp Electrical Steel, 62330 Isbergues, France

ARTICLE INFO

Keywords:
Grain Oriented Electrical Steel (GOES)
Medium Frequency Transformer (MFT)
Solid-State Transformer (SST)
High power density

ABSTRACT

The increasing part of intermittent renewable energy requires significant modifications of the electric grid. The introduction of smart nodes, where the power transfer can be adjusted in real time in addition to the classical voltage change and the galvanic isolation, becomes an important asset for the grid balance. Transformers associated with power electronic converters can ensure this function; they are known generically as Solid-State Transformers (SST). Their high specific power also opens opportunities for railway application. SSTs can be operated at high frequencies (a few tens of kHz), with ferrite or nanocrystalline cores operating at low flux densities. The paper proposes a complementary approach that consists in using transformers built with grain oriented electrical steel (GOES) wound cores, operating at medium frequencies (few kHz) and high flux densities. The reported work focuses on experimental assessment aiming to show that this option is now open for designing SST cells, which can be associated to reach bigger units.

1. Introduction

The complexity of the electric grid is increasing due to the growth of renewable intermittent energy sources (wind farms, solar plants, etc.). Solid State Transformers (SST) are relevant tools for ensuring flexible operations on the electric grid [1]. Most of the known SSTs are made of electronic converters, placed around High Frequency (HF) transformers, and a specific control system. To transfer high power, SSTs can be made of an association of fractional power SST cells [2, 3]. This concept can be used for smart grid applications [4] and in other domains such as renewable energy or railway traction [5]. The first SST demonstrator for a $16^{2/3}\,Hz$, $15kV$ railway applications was commissioned and installed on a test locomotive by ABB [6]. To cope with high voltage, cascading of several SST cells is necessary [7, 8, 9]. Multi-level high-frequency link for medium-voltage cascade converters has been also studied for renewable energy production systems and smart grid applications [10]. Metglas amorphous alloy is used in high frequency SSTs for building insulated balanced multiple DC supplies for medium voltages [11]. Nanocrystaline core material is also used for the design of a 35 kVA medium frequency transformer [12].

The need for, reliability and efficiency of SSTs is becoming higher and higher [13, 14]. The main challenges are the design of high power units in small volumes with high reliabilities at reasonable costs. Various types of material are used for the medium frequency transformer cores. For example the ability to stabilise the grid using a wind turbine generator was reported as to involve a connection through an amorphous 1.26 kVA transformer [11]. The design approach consists then in finding the best possible balance between the wound core geometry, the winding design, the topology of the power electronic converters and the control algorithm. Three DC/DC converter topologies suitable for high-power density high-power applications have been presented on the basis of a phase-shift control strategy [15] .

Transformers cores built with thin grain oriented electrical steel (GOES) offer an alternative solution for medium frequency transformers for SST. They can withstand high flux density levels (the saturation polarisation is 2.03 T) for several kHz. They can also be operated with simple power electronic topologies delivering square voltages. A single phase transformer can use a wound core architecture. The grain oriented steel is thus magnetised along its easy magnetisation direction, this means low loss and low scattering of the magnetic field.

GOES sheets have a mineral coating that can withstand high temperatures, the core can be operated up to 500°C without any significant reduction in magnetisation ability [16]. At high temperature the natural increase of resistivity reduces eddy currents losses. The paper deals with experimental assessments of a high-power SST cell made with a medium frequency transformer (MFT) based on a GOES wound core associated to standard IGBT converters. The main goal is to check the feasibility of this solution, considering that for reaching high power units, the SSTs capabilities to operate with high voltage levels and its global thermal balance are the main stakes.

2. SST Modular structure

Identical SST cells can be assembled together for building high power SSTs. In the reported work, each elementary cell contains two reversible single-phase converters and a MFT ensuring the galvanic insulation and the voltage change. The cells are connected in series on the high voltage (HV) side and in parallel for the low voltage (LV) side as illustrated in Fig. 1.

*First author
houssam.ichou@univ-artois.fr (H. Ichou)
ORCID(s): 0000-0003-4396-0952 (H. Ichou)

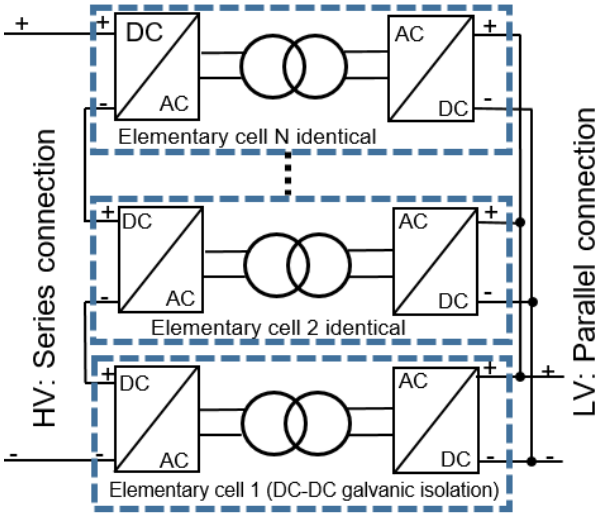

Figure 1: Modular structure of a high power SST.

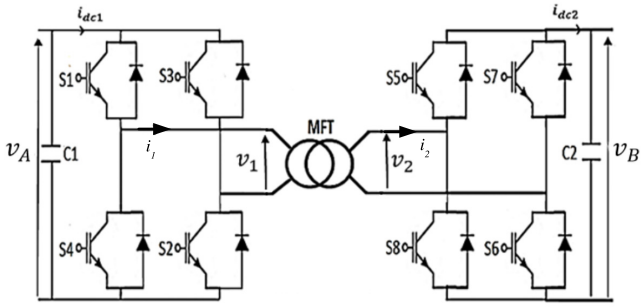

Figure 2: Detailed structure of an SST cell.

Two types of voltages must be considered: the differential mode defined for each MFT winding and the common-mode one defined between a winding terminal and the ground connection.

Figure 1 shows that the elementary cells connected in parallel have no specific common-mode insulation issues: the common-mode voltage is similar to the differential one. It is not the case for the series connection, which adds together the successive differential voltages of each converter. The top stack transformer is submitted to the full DC high voltage as common-mode stress. The other elementary cells of the stack receive a lower common-mode voltage, which is only a part of the high DC voltage.

The detailed power circuit of SST cell is presented in figure 2, this topology is known as Dual Active Bridge (DAB) meant to be operated using PSM. The command is designed for producing rectangular voltages shifted by certain adjustable time difference which is used for controlling the power flow. With such a basic command, the switching losses are reduced to their strict minimum for the required operating frequency.

Insulation issues must be considered keeping the general safety rules in mind. One of the most important is the connection to ground of all the metallic parts of any electric equipment. Consequently, the MFT core is grounded. Another rule consists in fixing the potential of the SST input and output terminals relatively to the ground. For many DC applications, the common-mode voltage depends on the neutral point connection of the feeding machine (transformer or alternator) and the rectifier design. The ground potential is often used as a middle point; therefore, the common mode voltages are in the order of half the differential ones. For traction applications with a DC grid the common-mode voltages are larger because the + is the catenary and the − the rail connected to the ground. The SST common-mode voltages are similar to differential ones. The SST insulation should be designed for this worst case. For each SST cell, the converters of the HV side must be placed inside insulated racks able to withstand the common-mode voltage stress. Optical fibres ensure the transmission of the digital command signals in order to provide a full galvanic insulation of the converters.

The global two steps project consists in developing cells for a modular structure that can be applied to railway traction with a $25kV_{rms}/50Hz$ catenary. It is organised as follows :
- The design and tests of a first elementary cell with a limited $30kV$ common-mode insulation capability. It uses a common-mode insulation based on air layers having the adequate thicknesses. This first release is aimed at gaining experience for then improving the MFT power density using a GOES wound core associated to a regular coil manufacturing process.
- The second elementary cell will be based on the experience gained from the first one. This elementary cell will offer a common-mode insulation capability up to $60kV$ and a higher power rating thanks to a specific topology and a more sophisticated insulation technology capable of low insulation distances and leakage inductances.

3. General topology of the MFT with a wound GOES core and a common-mode insulation at $30kV$

For a $30kV_{peak}$ common-mode insulation voltage, the critical distances of air can be predicted using the Paschen curve of Fig.3 plotted for dry air at ambient temperature. At sea-level pressure ($10^5 Pa$), the distance that creates the ionisation of air between flat electrode that have a potential difference of $30kV_{RMS}$ is $12mm$. Safety margins must be applied because the electric field lines in air are not straight lines as in Paschen's theory. The safety margin must be larger for the critical distance between the coil and the core because of the core edges.

The general topology of the transformer with large air gaps between the primary coil and the other parts of the transformer comes from this constraint. Figure 4 presents the choices made for the first system. The critical air gaps of the Electrical Insulation System (EIS) are $d_1 = 18mm$ and $d_2 = 20mm$. This, combined to the needed room for winding the conductors, induces the GOES wound core sizes

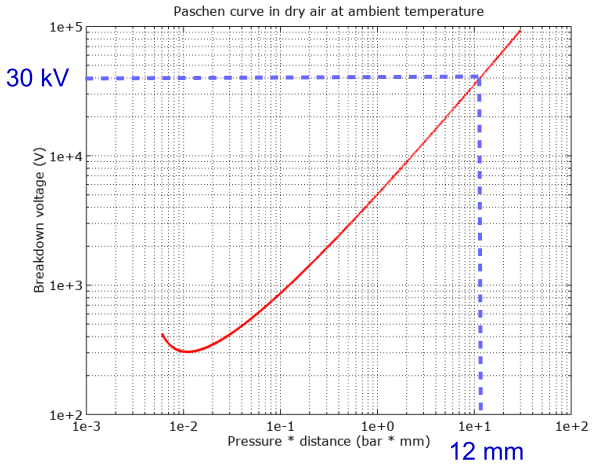

Figure 3: Paschen curve for dry air at room temperature.

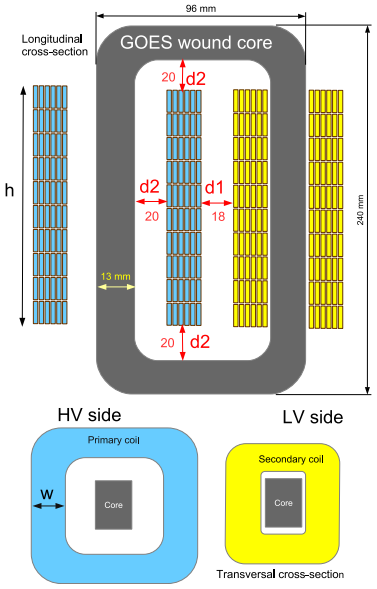

Figure 4: MFT topology with large insulation distances around the HV coil.

(240×96mm). These choices impose the leakage inductance value and consequently the maximum transmittable power at a given frequency. At 3kHz, the skin depth in copper is 1.47mm. A flat enamelled wire of $14 \times 2mm$ has then been used. For rectangular waveforms provided by the DC/AC converters, the RMS voltage of each coil is given by (1) where N is the number of turns of the considered coil, A_C the core cross-section area, B_m the maximum flux density in the core and f the frequency.

$$V_{rms} = 4 N A_C B_m f \quad (1)$$

The MFT core is made of wound GOES. The general data are given in Table. 1; voltages and currents are seek to be as high as possible.

The stress applied resulting form the wound core manufacturing process has been released through an appropriate annealing thermal cycle. The core is made of two halves for an easy placement of coils. The pole faces have been worked out to ensure minimum air-gap. Fig.5 shows the core before and after the cutting operation.

Two coils of 6 layers with 10 turn of $14 \times 2mm$ copper wire each have been implemented. Fig. 6 is a picture of the SST cell. The MFT is centred in between the two power electronic converters. The HV coil is bigger than the LV one because of the insulating distances.

Table 1
Main specifications used to build the experimental setup

Description	Sym.	Value
Number of primary windings	N_1	60
Number of secondary windings	N_2	60
Enamelled copper wire		$14 \times 2\ mm$
Operating frequency	f	1-3 kHz
Core cross section	A_C	5.93 cm^2
Core mean length	L_C	620 mm
Goes wound core mass	M_C	2.94 kg
Transformer weight	M	14 kg
Transformer volume	V	1.6 dm^3

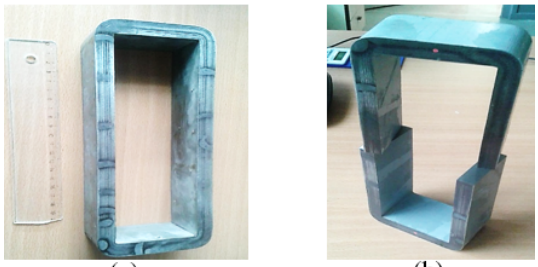

Figure 5: GOES wound core before and after the cutting process.

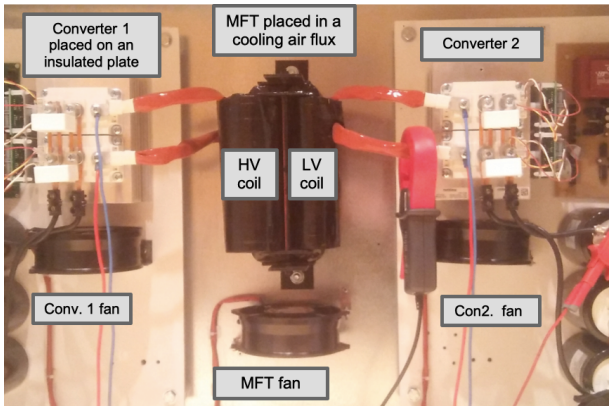

Figure 6: SST cell prototype including two converters and the MFT built with a HV coil made with the required insulation distances.

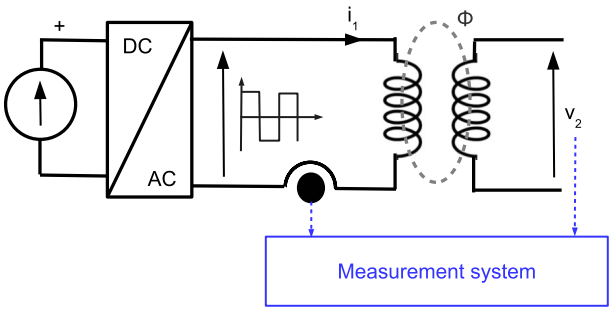

Figure 7: Core losses measurement system with square voltages.

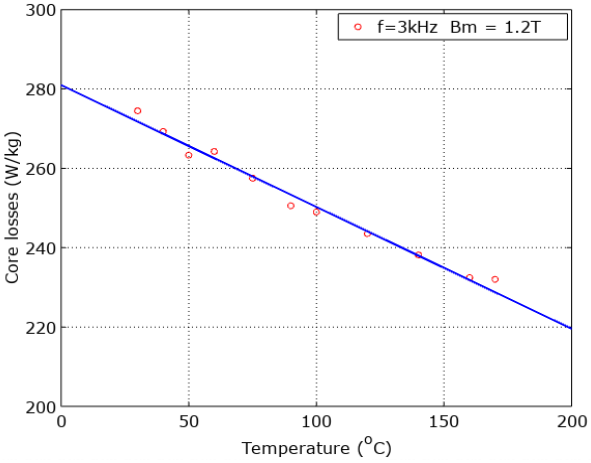

Figure 8: Core losses variation versus temperature and linear interpolation.

4. Core losses

For designing the MFT, the knowledge of the core losses are of utmost importance. Experimental investigations are made at medium frequencies under rectangular voltages with the measurement system presented in figure 7.

A study made on similar MFT [17] shows that the core losses are slightly lower for square voltage wave than for sine ones at the same peak flux density and frequency. Consequently, information about measurement of losses made with square waves is mandatory prior to perform a proper design of the transformer, prediction with sinusoidal waveforms is not relevant.

The voltage source is a H-bridge inverter, associated to a micro controller that imposes strictly a 50% duty cycle for avoiding any DC component. The peak value of the flux density in the core is tuned by acting on the DC input voltage of the inverter.

A broadband current probe collects the primary current wave form $i_1(t)$ for computing the magnetic field in the core according to the Ampere's law $N_1 i_1(t) = H(t).l_C$. The voltage induced in the secondary coil yields the flux density $B(t)$ by integration. The core losses are computed by (2).

$$P = \frac{1}{T}\frac{N_1}{N_2}\int_0^T i_1(t).v_2(t)\,dt \tag{2}$$

In spite of precaution taken to get rid of the burrs at the pole faces, additional losses did nevertheless took place. Stress and other factors still to be known may contribute also to this phenomenon.

GOES laminations are insulated from each other thanks to the double layer mineral coating which is intrinsic to the production process of the steel; its maximum thickness is 5 μm [18]. Their density and resistivity are respectively 7650 kg/m^3 and 0.48 $\mu\Omega m$. Core losses have been measured at different temperature values in a range of 30 °C to 170 °C and for $f = 3kHz$ and $B_m = 1.2\ T$. Figure 8 shows that core losses decrease significantly with the temperature. For these measurements, the magnetising current is 8 A_{RMS} at room temperature; it decreases slightly (5 %) when the temperature increases. This figure shows that the GOES core temperature is not itself an issue, but the coil temperatures increase because of the thermal flux produced by the core. The coil temperature must remain under the EIS thermal class.

At medium frequencies the core losses are mainly due to eddy currents [19] [20]. Consequently, when the core operates at high temperatures, the natural increase of GOES resistivity lowers eddy current losses, which has a global positive effect on the MFT efficiency.

5. Copper losses

Because of skin and proximity effects, the AC resistance of the coils depends on frequency. Copper losses are computed using AC resistance experimental curves measured with an impedance analyser at the MFT primary and secondary, at the operating frequency, when the other coil is short-circuited. The copper losses in each coil are computed with 3 and 4 using the resistance at the coil operating temperature. With the core losses determined experimentally, they make the 3 inputs of the thermal model aimed at computing the temperature of the main transformer parts.

$$P_P = R_{HV}(T_P) \cdot I_{1rms}^2 \tag{3}$$

$$P_S = R_{LV}(T_S) \cdot I_{2rms}^2 \tag{4}$$

The maximum power that can be transferred by the system and its efficiency are determined with the thermal model considering the thermal class of the EIS. In this model, the AC resistance increase of each coil with the temperature must be considered.

6. MFT thermal model

For standard organic insulation technologies relying on polymers, the maximum temperature is defined by the thermal class, which is the operating temperature for a life expectancy of 20000 h. The most common classes are F (155°C),

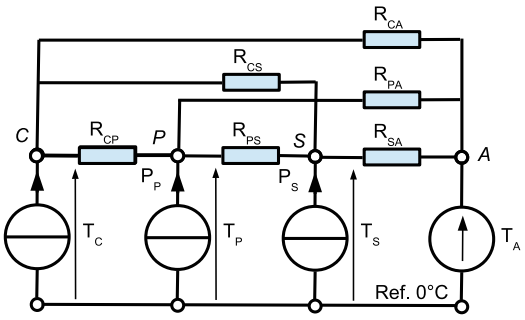

Figure 9: Thermal equivalent circuit.

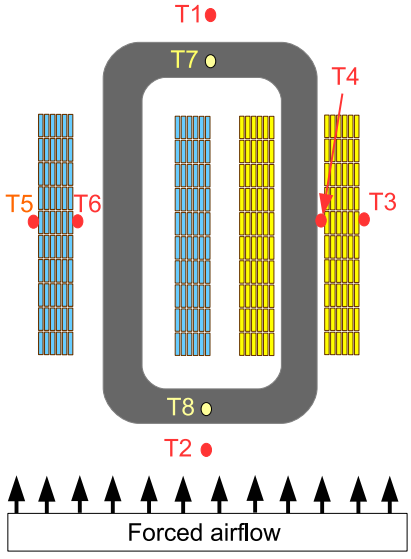

Figure 10: Location of the various thermocouples for the measurement of temperatures T1 to T8.

H (180°C), and C (200°C). Consequently, for obtaining a high specific power, the thermal management is mandatory. The MFT is placed vertically in a forced air flow generated by a fan located beneath the transformer.

The steady-state thermal model is shown in Fig. 9 based on three assumptions:
- Losses are uniformly distributed inside the volume of each MFT element (core, primary coil and secondary coil).
- The temperature is supposed to be uniform within each element. With this hypothesis the equivalent thermal circuit is reduced to 4 nodes: one for the core, one for each coil and one for the ambient airflow.
-Thermal resistance values are supposed to be constant whatever the temperature is (linear model); they must be computed for temperatures in the same range of operating ones.

Figure 10 shows the position of the temperature sensors used for experiments.

The nodes T_C, T_P, T_S, and T_A are the respectively the average temperatures of the core ($T7, T8$), the primary coil ($T5, T6$), the secondary one ($T3, T4$) and the ambient air ($T1, T2$). The power sources P_C, P_P and P_S stand for the losses in the core, the primary coil, secondary one. The thermal resistances of figure 9 model the thermal transfers between nodes.

The no-load test, which provides only core losses, corresponds to the maximum temperature differences between the two experimental test points of each TMF element. Results of table 2 show a small difference between the temperatures measured at the two test point of the same transformer element. However, the thermal gradient inside the secondary coil is higher because its inner face is very close to the core; the temperature difference between the test points remains low (12°C). The six thermal resistance values in table 3 are computed considering the MFT geometry and experiments.

Table 2
Temperatures for a no-load test.

Core (^oC)	Primary (^oC)	Secondary (^oC)	Ambient (^oC)
$T_7 = 129$ $T_8 = 122$	$T_5 = 62$ $T_6 = 69$	$T_3 = 69$ $T_4 = 81$	$T_1 = 24$ $T_2 = 23$
$T_C = 125.5$	$T_P = 65.5$	$T_S = 75$	$T_A = 23.5$

Table 3
Thermal resistance predicted values.

R_{CA} (K/W)	R_{PA} (K/W)	R_{SA} (K/W)	R_{CP} (K/W)	R_{CS} (K/W)	R_{PS} (K/W)
1	0.4	0.5	0.6	0.45	3

Noting $G = 1/R$ the thermal conductances (W/K), the equivalent circuit can be described by (5).

$$P_{loss} = AT - BT_A \tag{5}$$

$$\text{With : } P_{loss} = \begin{bmatrix} P_C \\ P_P \\ P_S \end{bmatrix}; T = \begin{bmatrix} T_C \\ T_P \\ T_P \end{bmatrix}; B = \begin{bmatrix} G_{CA} \\ G_{PA} \\ G_{SA} \end{bmatrix}$$

$$A = \begin{bmatrix} G_{CS} + G_{CA} + G_{CP} & -G_{CP} & -G_{CS} \\ -G_{CP} & G_{CP} + G_{PA} + G_{PS} & -G_{PS} \\ -G_{CS} & -G_{PS} & G_{PS} + G_{CS} + G_{SA} \end{bmatrix}$$

The temperatures at different parts of the transformer are expressed by (6).

$$T = A^{-1}.(P_{loss} + B.T_A) \tag{6}$$

The flowchart of Figure 11 details the procedure used for predicting the temperatures at each node. Figures 12 and

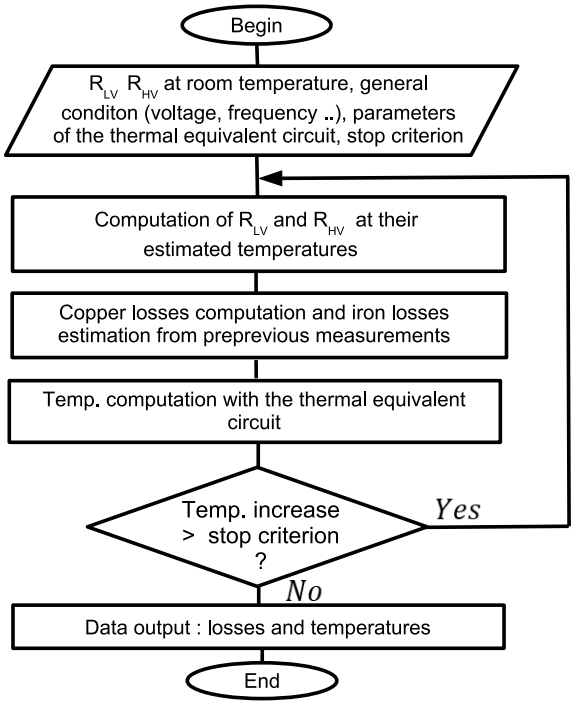

Figure 11: Flowchart for computing the MFT losses and nodes temperatures.

13 plot the results for temperatures and losses versus the secondary current for a voltage corresponding to the global tests presented in the next section. The operating frequency has been set to 2kHz for operating at coil temperatures compatibles with the insulation class or the TMF prototype. The core losses are predicted using the linear extrapolation of measurements presented in section 4. At medium frequencies, eddy current losses in GOES wound cores are dominant, it is then assumed that core losses depend on the square of the frequency [17]. Considering the experimental curve measured at $f_0 = 3kHz$, the core losses at the frequency $f_1 = 2kHz$ are predicted applying the ratio $(f_1/f_0)^2$.

It can be seen that, for low secondary currents, the coil temperatures are influenced by the core one. At higher currents, the copper losses have a major influence. Figure 13 shows the prediction of losses in each TMF element versus secondary current. It shows a slight reduction of core losses at high current because of the core temperature increase. However, the copper losses becomes dominant. Losses are higher in the primary coil because of its higher resistance due to its higher diameter.

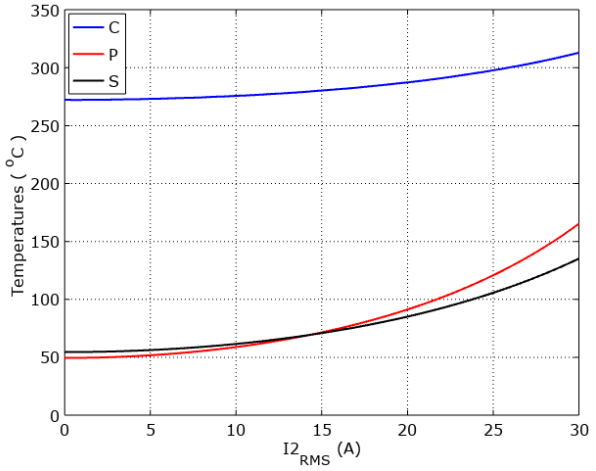

Figure 12: Prediction of internal temperatures versus secondary current for a wound GOES core operating at $1.2T_{peak}/2kHz$.

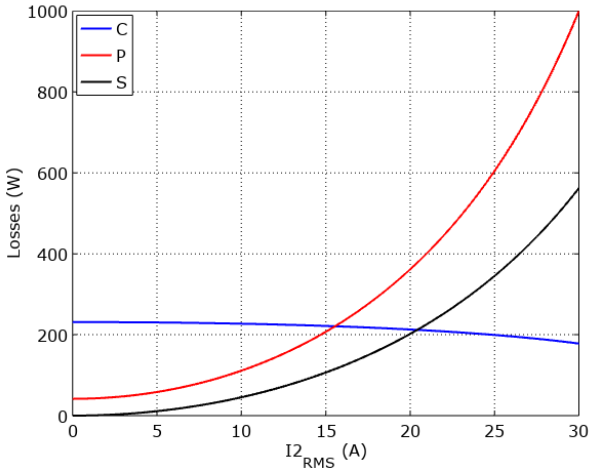

Figure 13: Prediction of losses versus secondary current for the same voltage and frequency.

7. Tests of the SST elementary cell

For analysing the cell behaviour, test have been made at 350 V DC / 2 kHz. The back-to-back system of figure 14 is used for simulating two DC grids. The power transfer is adjusted by the phase shift between the converter commands. Fig. 15 presents the voltage and current waveforms for a phase shift of 90°. This figure shows that the current increasing and decreasing slopes are limited by the leakage inductance when $v_1 \neq v_2$ the slight decrease when $v_1 = v_2$ is due to the global AC resistance of the circuit.

For this operating point, the core temperature and the currents are reported in table 4. With such a basic command, power factor of the TMF is not good; this drawback can be easily improved using a 3-level command for the converters. However, the back to back test proves that the GOES wound core MFT can be used for a large apparent power in a small volume when the global thermal balance allow a core at a

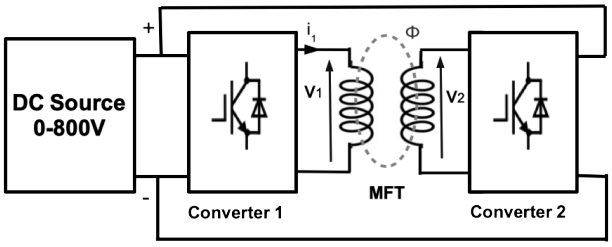

Figure 14: Back to back configuration.

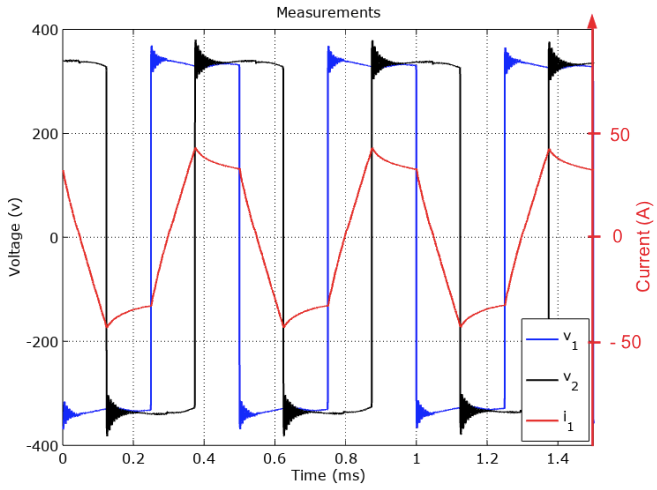

Figure 15: Example of voltage and current waveforms for a basic command .

higher temperature than coils.

Table 4
Main results for $f = 2kHz$ and $V_A = V_B = 350V$.

T_C ($^\circ C$)	T_P ($^\circ C$)	T_S ($^\circ C$)	Sec. current (A_{RMS})	App Power (kVA)
320	160	150	30.2	10.6

8. Conclusion

The concept of a SST cell using a medium frequency transformer (MFT) made with a grain-oriented electrical steel (GOES) wound core has been presented. This concept can makes sense for high power SSTs, which implies high voltage capabilities. The proposed SST cell is based on standard winding technology, made with rectangular enameled wire, and a common mode voltage insulation based on air layers with adequate thicknesses. The analysed structure showed the possibility for a core to be operated at quite high temperature for the sake of a high specific power and keeping the winding within its isolation class. In these conditions, a special care must be paid to the thermal balance of the whole MFT. The paper provides a nodal thermal equivalent circuit adapted to the MFT proposed topology.

Experience has been gained and is currently considered for the currently design of a new SST release :
- Adding thin thermal insulation layers, made of adapted material, between the core and the coils.
- Use of a high breakdown voltage polymer and electrostatic screens to lower insulation distances.
- Change windings for flat coils and Litz wires for lower resistance and leakage inductance.
- Adapt the command for improved power factor.

Acknowledgment

This work is funded by thyssenkrupp Electrical Steel.

References

[1] J. E. Huber and J. W. Kolar, "Volume/weight/cost comparison of a 1mva 10 kv/400 v solid-state against a conventional low-frequency distribution transformer," in *2014 IEEE Energy Conversion Congress and Exposition (ECCE)*. IEEE, 2014, pp. 4545–4552.

[2] D. S. Oliveira, D. d. A. Honório, L. H. S. Barreto, P. P. Praça, A. Kunzea, and S. Carvalho, "A two-stage ac/dc sst based on modular multilevel converterfeasible to ac railway systems," in *2014 IEEE Applied Power Electronics Conference and Exposition-APEC 2014*. IEEE, 2014, pp. 1894–1901.

[3] M. Glinka and R. Marquardt, "A new ac/ac multilevel converter family," *IEEE Transactions on Industrial Electronics*, vol. 52, no. 3, pp. 662–669, 2005.

[4] F. Vaca-Urbano and M. S. Alvarez-Alvarado, "Power quality with solid state transformer integrated smart-grids," in *2017 IEEE PES Innovative Smart Grid Technologies Conference-Latin America (ISGT Latin America)*. IEEE, 2017, pp. 1–6.

[5] C. Zhao, D. Dujic, A. Mester, J. K. Steinke, M. Weiss, S. Lewdeni-Schmid, T. Chaudhuri, and P. Stefanutti, "Power electronic traction transformer—medium voltage prototype," *IEEE Transactions on Industrial Electronics*, vol. 61, no. 7, pp. 3257–3268, 2013.

[6] M. Claessens, D. Dujic, F. Canales, J. K. Steinke, P. Stefanutti, and C. Vetterli, "Traction transformation," *ABB review*, vol. 1, no. 12, pp. 11–17, 2012.

[7] A. Rufer, N. Schibli, C. Chabert, and C. Zimmermann, "Configurable front-end converters for multicurrent locomotives operated on 16 2/3 hz ac and 3 kv dc systems," *IEEE Transactions on Power Electronics*, vol. 18, no. 5, pp. 1186–1193, 2003.

[8] M. Steiner and H. Reinold, "Medium frequency topology in railway applications," in *2007 European Conference on Power Electronics and Applications*. IEEE, 2007, pp. 1–10.

[9] H. Iman-Eini, S. Farhangi, J.-L. Schanen, and M. Khakbazan-Fard, "modular power electronic transformer based on a cascaded h-bridge multilevel converter," *Electric Power Systems Research*, vol. 79, no. 12, pp. 1625–1637, 2009.

[10] M. R. Islam, Y. Guo, and J. Zhu, "A high-frequency link multilevel cascaded medium-voltage converter for direct grid integration of renewable energy systems," *IEEE Transactions on Power Electronics*, vol. 29, no. 8, pp. 4167–4182, 2013.

[11] M. R. islam, Y. Guo, and J. Zhu, "A medium frequency transformer with multiple secondary windings for medium voltage converter based wind turbine power generating systems," *Journal of Applied Physics*, vol. 113, no. 17, p. 17A324, 2013.

[12] S. Balci, I. Sefa, and N. Altin, "Design and analysis of a 35 kva medium frequency power transformer with the nanocrystalline core material," *International Journal of Hydrogen Energy*, vol. 42, no. 28, pp. 17 895–17 909, 2017.

[13] D. Dujic, F. Kieferndorf, and F. Canales, "Power electronic transformer technology for traction applications–an overview," *Electronics*, vol. 16, no. 1, pp. 50–56, 2012.

[14] K. Wang, Q. Lei, and C. Liu, "Methodology of reliability and power density analysis of sst topologies," in *2017 IEEE Applied Power Electronics Conference and Exposition (APEC)*. IEEE, 2017, pp. 1851–1856.

[15] R. W. De Doncker, D. M. Divan, and M. H. Kheraluwala, "A three-phase soft-switched high-power-density dc/dc converter for high-power applications," *IEEE transactions on industry applications*, vol. 27, no. 1, pp. 63–73, 1991.

[16] M. Ababsa, O. Ninet, G. Velu, and J. Lecointe, "High-temperature magnetic characterization using an adapted epstein frame," *IEEE Transactions on Magnetics*, vol. 54, no. 6, pp. 1–6, 2018.

[17] S. Hamdinou, "Potential of grain-oriented electrical steels for the production of compact transformers with high power density," *Ph. D. thessis,*, Artois University, 11 Dec. 2019.

[18] R. Lemaître and T. Belgrand, "Matériaux magnétiques doux cristallins. acier électrique à grains orientés." *Techniques de l'ingénieur*, 2014.

[19] G. Bertotti, "General properties of power losses in soft ferromagnetic materials," *IEEE Transactions on magnetics*, vol. 24, no. 1, pp. 621–630, 1988.

[20] V. Basso, G. Bertotti, O. Bottauscio, F. Fiorillo, M. Pasquale, M. Chiampi, and M. Repetto, "Power losses in magnetic laminations with hysteresis: Finite element modeling and experimental validation," *Journal of applied physics*, vol. 81, no. 8, pp. 5606–5608, 1997.

Houssam Ichou received his master degree in physics and energy engineering from the university of Paris-Saclay in 2016. In 2017 he joined the Electrotechnical Systems and Environment Laboratory (LSEE) of the University of Artois in Bethune (France) as an engineer. Currently, he is a doctoral student in the department of electrical engineering at the university of Artois, Bethune, France. Research deals with the study and design of a high-power solid-state transformer operating at medium frequency, intended for railway traction, using a thin grain oriented electrical steel. His research interests include magnetic material, power electronics, converter topologies and control systems.

Prof. Daniel ROGER (Emeritus professor at Artois University, CEng, IEEE Senior Member). After working in industry, in secondary education and in Lille University, he was hired as an associate professor in Artois University. He has been a professor since 2004 in the same university. He has been at the head of the electrical engineering department for 4 years and a member of the steering board of the University in charge of valorization of academic research for 6 years. He has a teaching experience in power electronics, electromagnetism and electrical machines at master level. He has supervised many Ph.D thesis. His research interests are electrical machines, winding solutions for motor fed by PWM inverters, Solid-State Transformers (SST) and high temperature machines for applications in aeronautics. He is the author of more than 130 communications and publications in international journals and conferences.

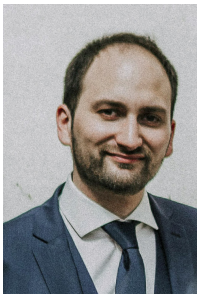

Dr. Mathieu ROSSI (Associate Professor at Artois University). After a Ph.D. in electrical engineering (2012) at the Ecole Centrale - Lille (France) and some years in industry (Transformers manufacturer, consulting company and freelance) he was hired as an associate professor in Artois University - France. His research interests are based on power transformers from low to high frequency. More precisely on problems like thermal modeling, acoustic noise, High voltage partial discharge and anisotropy on GOES sheets.

Dr. Thierry BELGRAND PhD in Material Science from University of Lille, started his carrier in Electrical steel in 1989 by integrating UGINE in Isbergues Plant (France). He launched there an Electrotechnical activity after spending a specialisation year under the lead of Pr. Brissonneau in Grenoble. In 1998, he moved to Stainless Steel activities in which he had various responsibilities in Quality control, Industrial projects, reengineering and change management. After a period in development for automotive industry, he took over the responsibility of tkES UGO *R&D* in 2007 then head of TKES Application Technology in 2014. He is expert to the IEC group related to measurement techniques of magnetic materials (TC68/WG2). Member of CIGRE, he is also member of the Scientific Committee of the French cluster MEDEE. He is now the expert for tkES in Electrotechnical fields of application for Grain Oriented Electrical steel and in charge of tkES Application Center.

Dr.-Ing. Régis LEMAÎTRE graduated engineer of ENS des Arts Métiers - (F) Paris in 1980, completed his PhD in Mechanical Engineering in 1982 and obtained in 1993 an executive MBA at the ICG-IFG - Lille (F). Activities in Electrical Steel for more than 30 years. He started first as process and quality engineer in (F) Isbergues plant - Usinor Group, became Head of the Electrical Steel Technical dept., later on of Customer Services and Final Production Operations. In 2004 he joined the Technology dept. of ThyssenKrupp Electrical Steel in Germany and became in 2007 Head of Research & Technology until 2017. His last position is VP Strategic Business Development at ThyssenKrupp Electrical Steel GmbH. Member of the IEC TC68 Standardization Committee for electrical steel properties, Vice-President of the French cluster MEDEE (Motors and Electrical Devices for Energy Efficiency).